# Contribution of Mesoscale Convective Complexes to Rainfall in Sahelian Africa: Estimates from Geostationary Infrared and Passive Microwave Data

ARLENE G. LAING*

*Cooperative Institute for Research in the Atmosphere, Colorado State University, Fort Collins, Colorado*

J. MICHAEL FRITSCH

*Department of Meteorology, The Pennsylvania State University, University Park, Pennsylvania*

ANDREW J. NEGRI

*Laboratory for Atmospheres, NASA/Goddard Space Flight Center, Greenbelt, Maryland*

(Manuscript received 10 March 1998, in final form 24 August 1998)

ABSTRACT

The contribution of mesoscale convective complexes to the July–September rainfall in Sahelian Africa is assessed using passive microwave data from the Special Sensor Microwave Image and infrared (IR) data from the European Geostationary Meteorological Satellite (Meteosat). A simple precipitation-estimation procedure, which takes advantage of the good time resolution of the IR and the strong relationship between the microwave radiance and rainfall, is developed and applied. The microwave technique uses the 37- and 86-GHz brightness temperatures to define the rain areas and the 86-GHz ice scattering signal to determine the rainfall intensity. The IR cloud shield areas are defined by the 219 K threshold.

Regression analyses are used to relate the microwave-derived precipitation characteristics of the system and the IR data closest to the time of the SSM/I observation. These relationships are used to compute the precipitation characteristics of the total set of systems and to determine their monthly rainfall contribution.

Results indicate that these systems have precipitation characteristics, such as rain area and volume, which are of the same order of magnitude as systems in the United States. In addition, they provide a significant fraction of the rainfall in Sahelian Africa.

## 1. Introduction

It has been shown that mesoscale convective systems (MCSs), of which mesoscale convective complexes (MCCs) are a significant subset, are the dominant warm season precipitation producing weather systems over the central United States (Fritsch et al. 1986). An enormous amount of rain can fall from MCCs; the average system produces between 3 and 9 km$^3$ of rainfall (Kane et al. 1987; McAnelly and Cotton 1989; Tollerud and Collander 1993). The rainfall from these systems benefits agriculture, but can also present a danger to life and property as occurred during the midwestern floods of 1993 (Scofield and Niameng 1994; Junker et al. 1995). In view of the importance of MCC-related precipitation in the United States, it is possible that MCCs will also contribute significantly to the rainfall in other regions. Indeed, similar systems have been responsible for devastating floods in East Asia (Ninomiya et al. 1981; Chen and Li 1995). This study estimates the rainfall characteristics of MCCs in Sahelian Africa, a region where systems that could be classified as MCCs or squall lines occur frequently (Aspliden et al. 1976; Payne and McGarry 1977; Desbois et al. 1988; Laing and Fritsch 1993; Rowell and Milford 1993).

Due to the lack of routine rain gauge measurements in these regions, it is necessary to use satellite data to estimate the rainfall. Despite considerable effort by investigators, rain gauge records are limited and mainly useful for monthly or annual climatic analyses, not for investigating mesoscale systems. While various studies have estimated rainfall from geosynchronous infrared (IR) and visible satellite data (Martin and Scherer 1973; Richards and Arkin 1981, Negri et al. 1984), these methods generally underestimate rainfall early and overestimate subsequent rainfall. With the IR measurements,

* Current affiliation: Department of Geography, University of South Florida, Tampa, Florida.

*Corresponding author address:* Dr. Arlene G. Laing, Department of Geography, University of South Florida, 4202 East Fowler Ave., SOC 107, Tampa, FL 33620.
E-mail: alaing@luna.cas.usf.edu

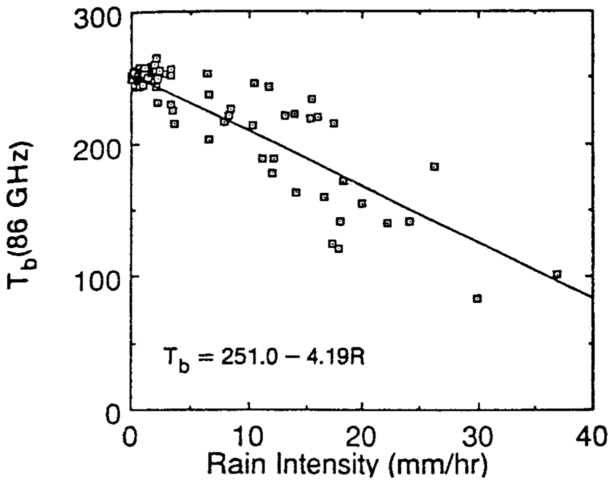


FIG. 1. Relation between brightness temperature at 86 GHz and rain rate derived from cloud model–microwave radiative model combination (from Adler et al. 1993).

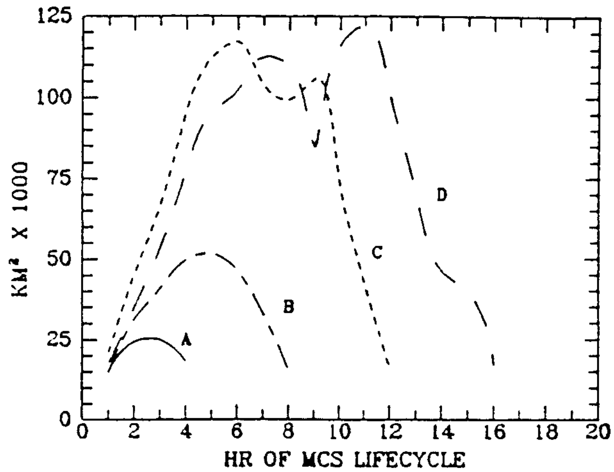


FIG. 2. Median −54°C cloud-top areas for each hour of the life cycles of MCSs that last (a) 4, (b) 8, (c), 12, and (d) 16 h (from Tollerud et al. 1992).

it is difficult to distinguish between precipitating and nonprecipitating cold-cloud tops and can lead to systematic errors in estimating rainfall.

The advent of the Defense Meteorological Satellite Program (DMSP) Special Sensor Microwave/Imager (SSM/I) brought fundamental change to the identification of precipitation from satellite because of the ability of the SSM/I to detect the microphysical properties of precipitating clouds (Spencer et al. 1989; Weng and Grody 1994). The SSM/I measures the microwave scattering and emission signatures of hydrometeors within clouds and has the fundamental advantage of relative insensitivity to cirrus clouds. Unfortunately, the SSM/I is on a low-orbit satellite, thereby limiting observations to one or two views per day. It may be possible, however, to develop a relationship between the SSM/I derived rainfall and simultaneous IR observations. Such a relationship could be used to improve the rainfall estimates from IR data alone. Since the IR data is much more frequently available, it would then be possible to make comprehensive estimates of African rainfall. The combination of the IR and microwave data has already resulted in improved rainfall estimates and simulations at other locations (Jobard and Desbois 1992; Adler et al. 1993, 1994; Karyampudi et al. 1993; Vicente and Anderson 1993).

## 2. Data and methodology

The SSM/I is mounted on the DMSP sunsynchronous polar orbiting satellite[1] with twice-a-day overpasses in Sahelian Africa (between 0430–0730 and 1630–1950 UTC) and a 12.5 km × 15 km footprint at 85.5 GHz. The microwave technique uses the brightness temperature at 37 and 85.5 GHz to define rain areas over land and water, and the 85.5 GHz scattering signal to define rain intensity (Fig. 1). More detailed description of the methods is given in Adler et al. (1993) and Wilheit et al. (1991). Digitized IR images from the European geostationary satellite (Meteosat) are used to identify and track the African MCCs through their life cycle. The images are products of the International Satellite Cloud Climatology Project (ISCCP) B3 state radiance (Schiffer and Rossow 1985) and have a spatial resolution of 30 km and temporal resolution of three synoptic hours.

The 3-h resolution of the available IR imagery made it difficult to determine the precise initiation and termination times of the MCC (definition given in Maddox, 1980). This limitation can be partially overcome 1) by assuming that the life cycle growth and decay rates of the African MCCs are similar to those in the United States [based on the similarity of characteristics documented in Laing and Fritsch (1993)], 2) matching the observed evolution of each African MCC IR area (−54°C) to the most similar growth/decay cycle of U.S. MCC IR areas (Fig. 2), and 3) extrapolating each similar growth/decay cycles to its initiation and termination times. The tracks of MCCs within the domain are shown in Fig. 3.

In order to utilize the more frequently available IR data to estimate precipitation, the following stepwise procedure was applied to correlate SSM/I rainfall data to IR data:

1) Both sets of observations are mapped to the same cylindrical map projection for ease of comparison.
2) For each MCC observed by the SSM/I, a normalized life cycle time of observation ($\tau$), that ranges from 0.0 to 1.0, is constructed. For example, the ‘‘normalized life cycle time’’ at two hours into the life cycle of an MCS that is observed to last eight hours

[1] 1987, the first year of the SSM/I, had a single imager and encountered problems with the 85-GHz vertical channel.

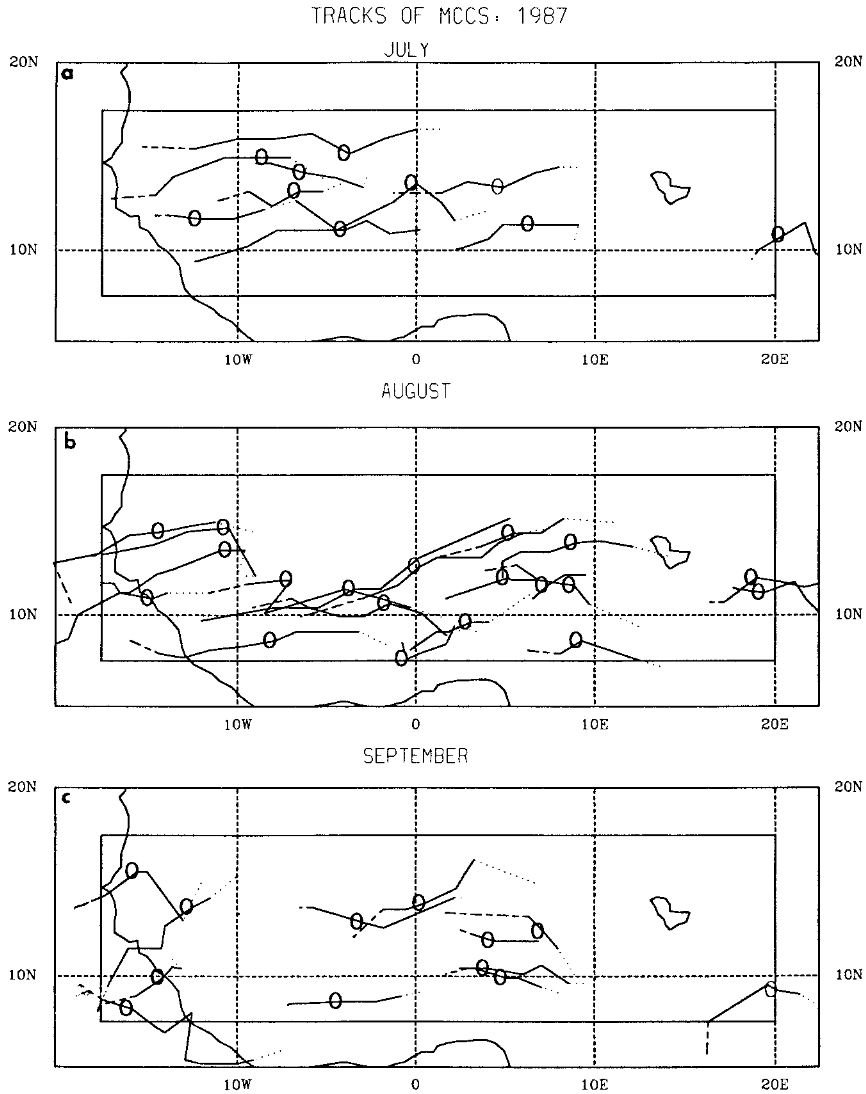


FIG. 3. Tracks of MCCs over Sahelian Africa during Jul–Sep 1987. Solid lines show the centroid locations from initiation to termination. Each track extends one observation point before initiation (dots) and after termination (dashes) with circles indicating centroid positions at maximum cold-cloud area.

is 0.25; for a system that lasts six hours, $\tau$ would be 0.33, etc.

3) The SSM/I-derived precipitation characteristics (e.g., rain area and rain rate) observed at the time $\tau$ are then correlated to the IR area observed at the time $\tau$ (see Fig. 4). In this manner, relationships are developed from which precipitation can be diagnosed using the IR-observed cold cloud area as a function of time of the MCC's life cycle.
4) The ratio of SSM/I-derived mean rain rate to IR area is plotted as a function of normalized life cycle time $\tau$ (see Fig. 5).
5) A best-fit polynomial curve is derived for the data points (Fig. 5). As an independent check on this least squares regression model, a similar plot (Fig. 6) was constructed using the results of McAnelly and Cotton's (1989) study (hereafter referred to as MC) of the precipitation of MCCs in the United States. It is clear that the two curves (Figs. 5 and 6) are very similar. Since the MC study used high-density surface rainfall observations and high frequency IR satellite images, the relationship shown in Fig. 5 appears very reasonable.

A similar methodology was used to determine the SSM/I rain area to IR area relationship (Figs. 7 and 8). The volumetric rate was calculated as a product of the instantaneous rain area and the area-averaged rain rate.

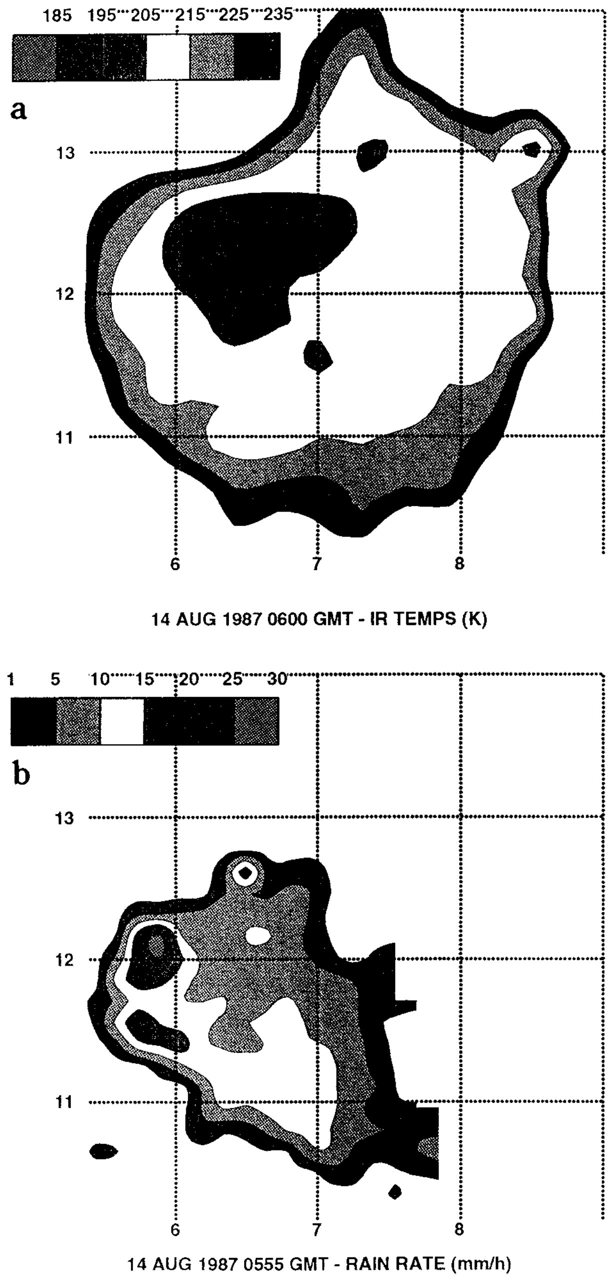


FIG. 4. Example of the same MCC observed by (a) geostationary IR and (b) SSM/I microwave.

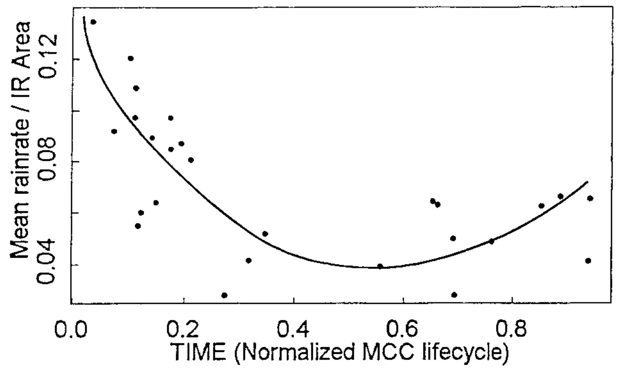


FIG. 5. Relationship between the mean rainrate to IR area ratio [(mm $h^{-1}$)(1000 $km^2$)$^{-1}$] and normalized time for African MCCs.

This volumetric rain rate was then used to compute the rainfall volume or total water from each system. Using the centroid locations, times, and instantaneous rain areas, the swath of rain produced over the lifetime of the system can be interpolated. By approximating each instantaneous rain area as a circle, it is fairly simple to assemble all the rainfall that occurs in each system. The assumption of circularity is justified by the a priori requirement that the aspect ratio of mature MCCs be greater than 0.7. The rainfall for each stage of the MCC life cycle was included as long as the centroid was within the domain, that is, more than 50% of the rain area was within the domain. Schematics in Fig. 9 illustrate how border cases are handled in the analysis.

Once individual system precipitation characteristics were computed, a summation over the 3-month period was performed to determine the accumulated rainfall from MCCs in this region. These results were then compared to the areal mean monthly precipitation from the Global Precipitation Climatology Project (GPCP) Combined Precipitation Data Set (Huffman et al. 1997; Fig. 10). In view of the strong gradient of rainfall across the domain and the geographic distribution of MCCs (cf. Figs. 3 and 10), MCCs in the northern part of the domain were examined separately. Grid latitude 12.5°N was used as the demarcation line between the different rainfall regimes because it was closest to the mean position of the 200-mm contour (Fig. 10). The southern part has more rainfall, fewer thunderstorms, and weaker ice-scattering signatures (Zipser 1994). In contrast, Mohr and Zipser (1996) observed strong 85-GHz and MCSs and MCCs within the arid regions of the north, a region bordering on the Sahara, where the MCC rainfall contribution may be very important.

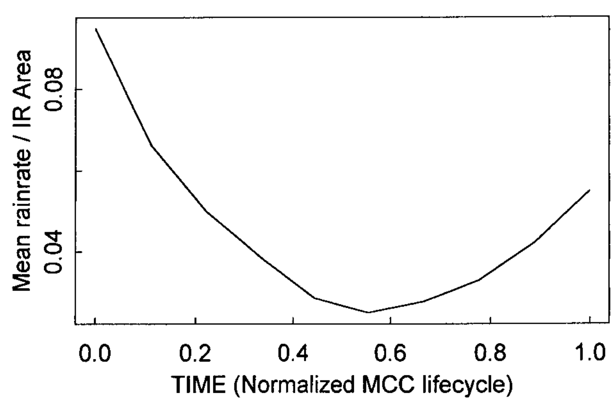


FIG. 6. Same as Fig. 5 but for U.S. MCCs.

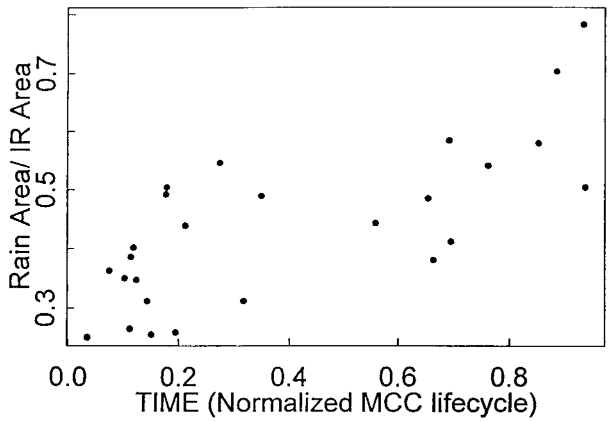


FIG. 7. Relationship between the mean rain area to IR area ratio and normalized time for African MCCs.

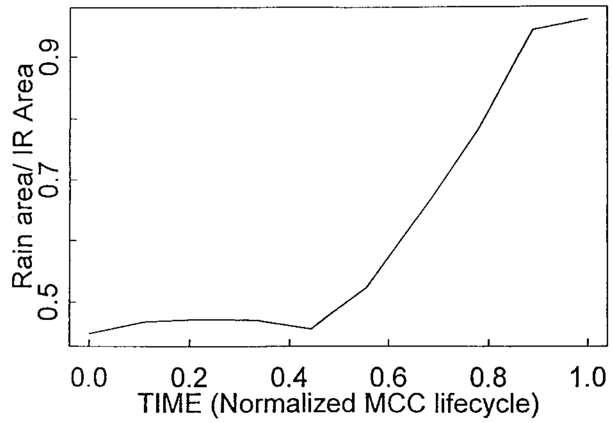


FIG. 8. Same as Fig. 7 but for U.S. MCCs.

## 3. Results

### *a. Precipitation characteristics of African MCCs*

The rainfall characteristics of 41 MCCs occurring over tropical north Africa during July–September 1987 were examined. The regression models derived from the methodology described in section 2 are

$$\text{Mean rain rate/IR area} = 0.119 - 0.258\tau + 0.217\tau^2$$

$$(R^2 = 0.563)$$

and

$$\text{Rain area/IR area} = 0.319 + 0.319\tau.$$

$$(R^2 = 0.544)$$

A summary of the rainfall characteristics of the MCCs observed is given in Table 1. The average volume of rainfall produced during the lifetime of African MCCs is more than twice that produced in the MC composite MCC. The average volume of rainfall is approximately three times the MC composite volume (3.46 $km^3$) but closer to the mean volume (8.23 $km^3$) calculated by Kane et al. (1987). The differences occurred because the SSM/I-derived rain rate is much greater than their composite rain rate (compare Figs. 5 and 6). The relatively poor sampling during the middle of the life cycle may have had an impact on the analysis. Another reason may be that the values illustrated in Figs. 4 and 8 of MC are derived from a composite, while in this study, the cumulative rainfall and volume from all systems were calculated, and then averaged for those values. However, the most likely reason is that the MC study included only hourly observing stations, whereas the Kane et al. (1987) analysis included a much greater number of stations and the SSM/I observes an area/volume (12.5 km $\times$ 15 km footprint) in total, rather than point gauge values.

### *b. Contribution to the total precipitation*

The MCCs contributed approximately 22% of the July–September rainfall in Sahelian Africa (see Table 2). For July, when only half a month of IR data was available for MCC documentation, the observed MCCs contributed over one quarter of the rainfall.

When the MCC contribution is examined with regard to the geographic distribution of monthly mean rainfall, the results are even more interesting (Table 3). In July, seven MCCs contributed 36% of the monthly mean rainfall north of 12.5°N while, during August, the wettest month, northern MCCs produced approximately 24% of the rainfall that region. The September systems accounted for 18% of the rainfall in the northern part of the domain, an increase over the total regional contribution. On average, MCCs contributed 26% of the rainfall in the northern part of the Sahel. Considering the distinctive nature of MCC rainfall in the United States where 20% of extreme rainfall is MCC related although they are only 7% of the observations (Tollerud and Collander 1993), the implications for flood potential may be as important in the Sahel.

The percentage contribution of MCCs to the monthly rainfall in this region may be somewhat conservative since the observed precipitation totals were in a region

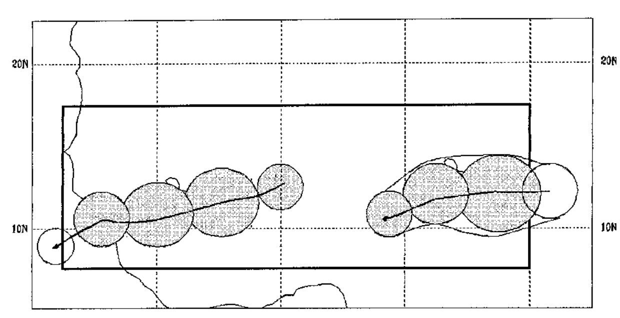


FIG. 9. Schematic representation of the rainfall swaths during the lifetime of Sahelian MCCs. Shading indicates areas that were included in the regional rainfall contribution.

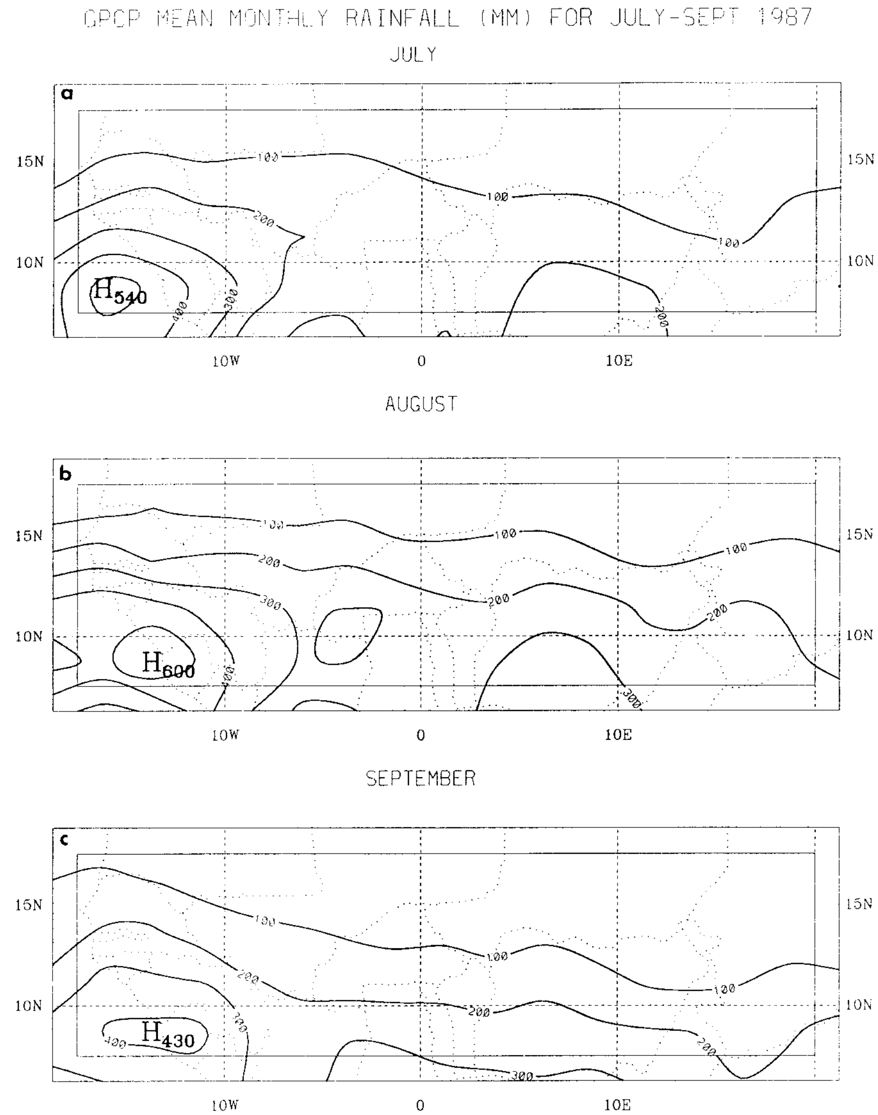


FIG. 10. Mean rainfall (in mm day⁻¹) for (a) Jul, (b) Aug, and (c) Sep 1987 for study region. Data are the GPCP combined satellite and gauge products.

with a relatively sparse rain gauge distribution (Global Precipitation Climatology Center 1992). Furthermore, the GPCP totals also include IR estimates, which are usually much greater than the actual rainfall.

## 4. Summary and concluding remarks

A relationship between SSM/I-derived precipitation characteristics and IR data was used to estimate the precipitation produced by African MCCs. The estimated volumetric rainfall amount from the average African system was larger than that of the average United States system, a result perhaps due in part to differences in observation method. The average area covered by rainfall during the lifetime of the system is comparable to that of similar systems in the United States and China.

It was found that MCCs contribute significantly to the rainfall in Sahelian Africa. Specifically, MCCs accounted for approximately 22% of the total rainfall during July–September 1987. Although MCCs were only documented for the second half of July, they produced one quarter of the monthly total and more than one-third of the rainfall in the arid northern sector. This is interesting because of the implications for tropical cyclone development; Gray and Landsea (1992) indicate

TABLE 1. Rainfall characteristics of Sahelian African MCCs during Jul–Sep 1987.

| No. of MCCs | Average rainfall (mm) | Average volume ($km^3$) | Average rain area ($km^2$) |
|---|---|---|---|
| 41 | 34 | 11.9 | 285 000 |

TABLE 2. Contribution of MCCs to monthly rainfall (GPCP combined data product) over Sahelian Africa, 7.5°–17.5°N, 17.5°W–20°E.

| Month | No. of MCCs | MCC volume (km³) | Region volume (km³) | Percentage contribution (volume) |
|---|---|---|---|---|
| Jul* | 10 | 164 | 657 | 25.0 |
| Aug | 19 | 257 | 955 | 27.0 |
| Sep | 12 | 70 | 645 | 10.8 |
| **Total** | **41** | **491** | **2258** | **21.7** |

* For MCCs occurring during 17–31 Jul 1987.

that there is a strong statistical relationship between early summer western Sahelian rainfall and the active Atlantic hurricane season. Moreover, diagnostic studies have documented that MCCs frequently produce balanced warm-core mesovortices (Menard and Fritsch 1989; Fritsch et al. 1994) and that MCCs have been the direct precursor to tropical cyclogenesis (Velasco and Fritsch 1987; Miller and Fritsch 1991; Laing and Fritsch 1993).

Although MCCs occur throughout the Sahel, they are clustered around a few longitudinal bands, and their rainfall contribution becomes even more important in those locations. Furthermore, the regional contribution could be significantly larger than estimated here since the GPCP monthly totals used as the baseline for comparison included IR estimates that are usually much greater than the actual rainfall (Adler et al. 1993, 1994).

These results are important because improvements in forecasting these systems would likely lead to improvements in predicting rainfall and runoff—information that is vital to the Sahelian region. Also, the significant contribution of MCCs to rainfall in certain regions (central United States and Sahelian Africa) and the large number of MCC occurrences worldwide (300–400 annually) indicate that their role in the global hydrologic cycle may be vital.

Finally, there are important methodological implications from this work. The rainfall estimation technique could be improved by extending the study for a longer period and incorporating higher resolution infrared observations. In addition, similar infrared-microwave algorithms could be developed for other regions that lack rain gauge measurements.

TABLE 3. Contribution of MCCs to monthly rainfall (GPCP combined data product) over the northern Sahel, 12.5°–17.5°N, 17.5°W–20°E.

| Month | No. of MCCs | MCC volume (km³) | North volume (km³) | Percentage contribution (volume) |
|---|---|---|---|---|
| Jul* | 7 | 61 | 167 | 36.5 |
| Aug | 8 | 59 | 248 | 23.8 |
| Sep | 5 | 25 | 138 | 18.1 |
| **Total** | **20** | **145** | **553** | **26.2** |

* For MCCs occurring during 17–31 Jul 1987.

*Acknowledgments.* We are grateful to Dr. George Huffman and Dr. Dave Randel for assistance with processing GPCP data. The ISCCP B3 data were provided by the NASA Langley Data and Acquisition Center and SSM/I data provided by the NASA Goddard Space Flight Center. This research was supported by NSF Grant ATM-92-22017.

REFERENCES

Adler, R. F., A. J. Negri, P. R. Keehn, and I. M. Hakkarinen, 1993: Estimation of monthly rainfall over Japan and surrounding waters from a combination of low-orbit microwave and geosynchronous IR data. *J. Appl. Meteor.,* **32,** 335–356.

——, G. J. Huffman, and P. R. Keehn, 1994: Global rain estimates from microwave-adjusted geosynchronous IR data. *Remote Sens. Rev.,* **11,** 125–152.

Aspliden, C. I., Y. Tourre, and J. B. Sabine, 1976: Some climatological aspects of West African disturbance lines during GATE. *Mon. Wea. Rev.,* **104,** 1029–1035.

Chen, Y.-L., and J. Li, 1995: Large-scale conditions favorable for the development of heavy rainfall during TAMEX IOP 3. *Mon. Wea. Rev.,* **123,** 2978–3002.

Desbois, M., T. Kayiranga, B. Gnamien, S. Guessous, and L. Picon, 1988: Characterization of some elements of the Sahelian climate and their inter-annual variations for July 1983, 1984, and 1985 from the analysis of METEOSAT ISCCP data. *J. Climate,* **1,** 867–904.

Fritsch, J. M., R. J. Kane, and C. R. Chelius, 1986: The contribution of mesoscale convective systems to the warm season precipitation in the United States. *J. Climate Appl. Meteor.,* **25,** 1333–1345.

——, J. D. Murphy, and J. S. Kain, 1994: Warm core vortex amplification over land. *J. Atmos. Sci.,* **51,** 1781–1806.

Global Precipitation Climatology Centre, 1992: Monthly precipitation estimates based on gauge measurements on the continents for the year 1987 (preliminary results) and future requirements. Rep. DWD/K&/WZN-1992/08-1, WMO/WCRP and DWD, Offenbach am Main, Germany, 20 pp.

Gray, W. M., and C. W. Landsea, 1992: African rainfall as a precursor of hurricane-related destruction on the U.S. East Coast. *Bull. Amer. Meteor. Soc.,* **73,** 1352–1364.

Huffman, G. J., and Coauthors, 1997: The Global Precipitation Climatology Project (GPCP) Combined Precipitation Data Set. *Bull. Amer. Meteor. Soc.,* **78,** 5–20.

Jobard, I., and M. Desbois, 1992: A method combining infrared and microwave satellite radiances for the estimation of the tropical rain. Preprints, *Sixth Conf. on Satellite Meteorology and Oceanography,* Atlanta, GA, Amer. Meteor. Soc., 264–267.

Junker, N. W., R. S. Scheidner, and R. A. Scofield, 1995: The meteorological conditions associated with the Great Midwest Flood of 1993. Preprints, *14th Conf. on Weather Analysis and Forecasting,* Dallas, TX, Amer. Meteor. Soc., 13–17.

Kane, R. J., C. R. Chelius, and J. M. Fritsch, 1987: Precipitation characteristics of mesoscale convective weather systems. *J. Climate Appl. Meteor.,* **26,** 1345–1356.

Karyampudi, V. M., J. Manobianco, S. Koch, G. Lai, A. J. Negri, and C. Kummerow, 1993: Simulations of Hurricane Florence with the assimilations of SSM/I and GOES/IR-derived rainfall rates. Preprints, *20th Conf. on Hurricanes and Tropical Meteorology,* San Antonio, TX, Amer. Meteor. Soc., 177–180.

Laing, A. G., and J. M. Fritsch, 1993: Mesoscale convective complexes over Africa. *Mon. Wea. Rev.,* **121,** 2254–2263.

Maddox, R. A., 1980: Mesoscale convective complexes. *Bull. Amer. Meteor. Soc.,* **61,** 1374–1387.

Martin, D. W., and W. D. Scherer, 1973: Review of satellite rainfall estimation methods. *Bull. Amer. Meteor. Soc.,* **54,** 661–674.

McAnelly, R., and W. M. Cotton, 1989: The precipitation lifecycle of mesoscale convective complexes over the central United States. *Mon. Wea. Rev.,* **117,** 784–807.

Menard, R. D., and J. M. Fritsch, 1989: An MCC-generated inertially stable warm core vortex. *Mon. Wea. Rev.,* **117,** 1237–1261.

Miller, D., and J. M. Fritsch, 1991: Mesoscale convective complexes in the western Pacific region. *Mon. Wea. Rev.,* **119,** 2978–2992.

Mohr, K. I., and E. J. Zipser, 1996: Mesoscale convective systems defined by their 85-GHz ice scattering signature: Size and intensity comparison over tropical oceans and continents. *Mon. Wea. Rev.,* **124,** 2417–2437.

Negri, A. J., R. F. Adler, and P. J. Wetzel, 1984: Satellite rain estimation: An analysis of the Griffith-Woodley technique. *J. Climate Appl. Meteor.,* **23,** 102–116.

Ninomiya, K., M. Ikawa, and T. Akiyama, 1981: Long-lived medium-scale cumulonimbus cluster in Asian subtropical humid region. *J. Meteor. Soc. Japan,* **59,** 564–577.

Payne, S. W., and M. M. McGarry, 1977: The relationship of satellite inferred convective activity to easterly wave over west Africa and the adjacent ocean during Phase III of GATE. *Mon. Wea. Rev.,* **105,** 413–420.

Richards, F., and P. Arkin, 1981: On the relationship between satellite cloud cover and precipitation. *Mon. Wea. Rev.,* **109,** 1081–1093.

Rowell, D. P., and J. R. Milford, 1993: On the generation of African squall lines. *J. Climate,* **6,** 1181–1193.

Schiffer, R. A., and W. B. Rossow, 1985: ISCCP global radiance data set: A new resource for climate research. *Bull. Amer. Meteor. Soc.,* **66,** 1498–1505.

Scofield, R. A., and L. Naimeng, 1994: The use of satellite imagery during the great floods of 1993. Preprints, *Seventh Conf. on Satellite Meteorology and Oceanography,* Monterey, CA, Amer. Meteor. Soc., 345–350.

Spencer, R. W., H. Michael Goodman, and R. E. Hood, 1989: Precipitation retrieval over land and ocean with the SSM/I: Identification and characteristics of the scattering signal. *J. Atmos. Oceanic Technol.,* **6,** 254–273.

Tollerud, E. I., and R. S. Collander, 1993: A 10-year synopsis of record station rainfall produced in mesoscale convective complexes. Preprints, *13th Conf. on Weather Analysis and Forecasting,* Vienna, VA, Amer. Meteor. Soc., 430–433.

——, J. A. Augustine, and B. D. Jamison, 1992: Cloud top characteristics of mesoscale convective systems in 1986. Preprints, *Sixth Conf. on Satellite Meteorology and Oceanography,* Atlanta, GA, Amer. Meteor. Soc., J3–J7.

Velasco, I., and J. M. Fritsch, 1987: Mesoscale convective complexes in the Americas. *J. Geophys. Res.,* **92,** 9591–9613.

Vicente, G. A., and J. R. Anderson, 1993: Retrieval of rainfall rates from the combination of passive microwave radiometric measurements and infrared measurements. Preprints, *20th Conf. on Hurricanes and Tropical Meteorology,* San Antonio, TX, Amer. Meteor. Soc., 151–153.

Weng, F., and N. C. Grody, 1994: Retrieval of cloud liquid water using the Special Sensor Microwave Imager (SSM/I). *J. Geophys. Res.,* **99,** 25 535–25 551.

Wilheit, T., A. Chang, and L. Chiu, 1991: Retrieval of monthly rainfall indices from microwave radiometric measurements using probability distribution function. *J. Atmos. Oceanic Technol.,* **8,** 118–136.

Zipser, E. J., 1994: Deep cumulus cloud systems in the Tropics with and without lightning. *Mon. Wea. Rev.,* **122,** 1837–1851.